



This is a repository copy of *High-occupancy effects and stimulation phenomena in semiconductor microcavities*.

White Rose Research Online URL for this paper:  
<http://eprints.whiterose.ac.uk/1470/>

---

**Article:**

Skolnick, M.S., Tartakovskii, A.I., Butte, R. et al. (2 more authors) (2002) High-occupancy effects and stimulation phenomena in semiconductor microcavities. *IEEE Journal of Selected Topics in Quantum Electronics*, 8 (5). pp. 1060-1071. ISSN 1077-260X

Doi:10.1109/JSTQE.2002.804234

---

**Reuse**

Unless indicated otherwise, fulltext items are protected by copyright with all rights reserved. The copyright exception in section 29 of the Copyright, Designs and Patents Act 1988 allows the making of a single copy solely for the purpose of non-commercial research or private study within the limits of fair dealing. The publisher or other rights-holder may allow further reproduction and re-use of this version - refer to the White Rose Research Online record for this item. Where records identify the publisher as the copyright holder, users can verify any specific terms of use on the publisher's website.

**Takedown**

If you consider content in White Rose Research Online to be in breach of UK law, please notify us by emailing [eprints@whiterose.ac.uk](mailto:eprints@whiterose.ac.uk) including the URL of the record and the reason for the withdrawal request.



[eprints@whiterose.ac.uk](mailto:eprints@whiterose.ac.uk)  
<https://eprints.whiterose.ac.uk/>

# High-Occupancy Effects and Stimulation Phenomena in Semiconductor Microcavities

M. S. Skolnick, Alexander I. Tartakovskii, Raphaël Butté, D. M. Whittaker, and R. Mark Stevenson

*Invited Paper*

**Abstract**—This paper describes recent work on high-occupancy effects in semiconductor microcavities, with emphasis on the variety of new physics and the potential for applications that has been demonstrated recently. It is shown that the ability to manipulate both exciton and photon properties, and how they interact together to form strongly coupled exciton–photon coupled modes, exciton polaritons, leads to a number of very interesting phenomena, which are either difficult or impossible to achieve in bulk semiconductors or quantum wells. The very low polariton density of states enables state occupancies greater than one to be easily achieved, and hence stimulation phenomena to be realized under conditions of resonant excitation. The particular form of the lower polariton dispersion curve in microcavities allows energy and momentum conserving polariton–polariton scattering under resonant excitation. Stimulated scattering of the bosonic quasi-particles occurs to the emitting state at the center of the Brillouin zone, and to a companion state at high wave vector. The stimulation phenomena lead to the formation of highly occupied states with macroscopic coherence in two specific regions of  $k$  space. The results are contrasted with phenomena that occur under conditions of nonresonant excitation. Prospects to achieve “polariton lasing” under nonresonant excitation, and high-gain, room-temperature ultrafast amplifiers and low-threshold optical parametric oscillator under resonant excitation conditions are discussed.

**Index Terms**—Lasing, microcavities, photonic structures, stimulated emission.

## I. INTRODUCTION

SEMICONDUCTOR microcavities are micrometer-scale photonic structures in which quantum wells are embedded within a high finesse Fabry–Pérot cavity, the whole structure being prepared by high precision, modern crystal growth techniques. Extensive reviews of the field are given in [1]–[4]. In such structures, vertical confinement of both excitons in the quantum wells and of light within the Fabry–Pérot cavity results in strong and controllable light-matter interactions unachievable in quantum wells or bulk semiconductors. This control has opened up a new field of exciton–polariton physics, where key features of the interacting exciton–photon system can be tailored by sample design. Most importantly for the

physics described here, the dispersion curves of the coupled two-dimensional (2-D) exciton–photon modes, exciton–polaritons (termed cavity polaritons), differ from those of their bulk analogs since the confinement of light results in a finite energy at  $k = 0$ . This property, combined with the controllable dispersion, the extremely low density of polariton states [1]–[4], and the bosonic character of the polariton quasi-particles have recently allowed a variety of new phenomena to be observed, including final state stimulation and a new condensed phase with macroscopic coherence, which have the potential to lead to new devices including very low threshold optical parametric oscillators, high-gain amplifiers, and a coherent light source based on stimulated polariton scattering.

A schematic diagram of a typical structure is shown in Fig. 1(a). The structure consists of a  $3\lambda/2$  GaAs cavity ( $\lambda$  is the wavelength of light in the medium) surrounded by 20 (below) and 17 (above) layers of  $\text{Al}_{0.13}\text{Ga}_{0.87}\text{As}$ –AlAs high reflectivity Bragg mirrors. The quantization of light in the vertical direction with free propagation within the plane leads to the approximately quadratic photon dispersion shown in Fig. 1(b). Two sets of three  $\text{In}_{0.06}\text{Ga}_{0.94}\text{As}$  quantum wells are embedded within the GaAs cavity and provide 2-D excitonic states, which are also confined in the vertical direction. Provided the broadenings of both the exciton and photon states are small compared to their characteristic interaction energy  $\Omega$  [see Fig. 1(b), the vacuum Rabi splitting  $\Omega$  is  $\sim 6$  meV for the sample investigated], the strong coupling limit [5] is achieved where new quasi-particles arise, termed cavity (exciton)–polaritons. As a result of the coupling, pronounced anticrossing of the exciton and cavity mode dispersions is observed, leading to the formation of new polariton branches with dispersion relations possessed by neither photons nor excitons alone [Fig. 1(b)]. Most notably, the lower polariton branch exhibits a dispersion which is photon-like at small wave vector and exciton-like at large wave vector, with a point of inflection in the dispersion between these two extremes, as shown in Fig. 1(b). It is this dispersion which leads to much of the new physics reported in the present paper. It gives rise to new energy and wave vector conserving scattering processes, it has a minimum at finite energy as opposed to the dispersion of polaritons in three dimensions, and its shape is controllable by changing the detuning  $\Delta$ , the energy separation between the uncoupled exciton and photon modes.

Manuscript received June 17, 2002; revised July 29, 2002. This work was supported in part by the Engineering and Physical Sciences Research Council (EPSRC) and in part by the European Community (EC) Project Clermont HPRN-CT-1999-00132.

The authors are with the Department of Physics and Astronomy, University of Sheffield, Sheffield S3 7RH, U.K.

Digital Object Identifier 10.1109/JSTQE.2002.804234

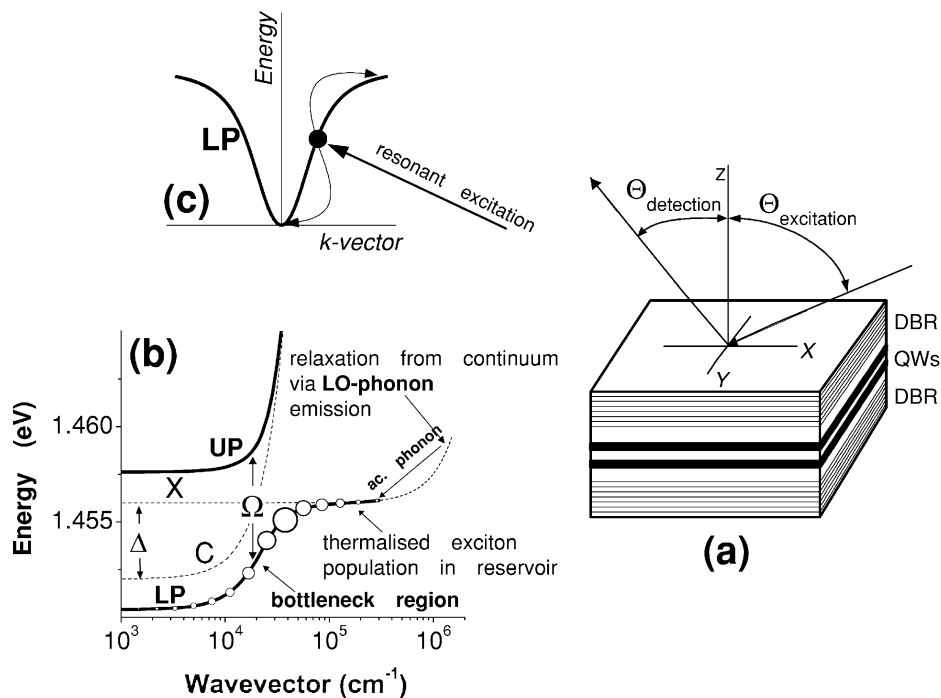


Fig. 1. (a) Schematic diagram of the sample and excitation/detection geometry. (b) Polariton (thick lines) and uncoupled cavity mode ( $C$ ) and exciton ( $X$ ) dispersions. The mechanisms responsible for relaxation following nonresonant excitation are indicated. The polariton population is represented schematically by the open symbols, with the maximum occurring at the edge of the polariton strongly coupled region. (c) Schematic diagram for resonant excitation into the polariton region.

Although the constituent electron–hole components of excitons have fermionic character, excitons have integer spin and are expected to exhibit bosonic properties. Since photons are bosons, exciton–photon coupled modes (polaritons) will also exhibit bosonic properties. For bosonic particles, large populations of individual states are allowed by their fundamental symmetry properties (as opposed to fermions which must obey the Pauli exclusion principle). Such macroscopic occupations for bosons and accompanying stimulation of transitions underly the phenomenon of Bose–Einstein condensation, and of photon stimulation in a laser. Since the rate for any quantum mechanical transition is proportional to  $(1 + N_{final})$ , where 1 describes spontaneous processes, and  $N_{final}$  describes stimulation of the transition by occupation of the final state, bosonic particles exhibit the property of stimulation of transitions by final state occupation. Such stimulation underlies the operation of lasers, where photon emission is stimulated by macroscopic occupation of the photon modes of the cavity. In this paper, we demonstrate stimulation of the scattering of polaritons, which in turn gives rise to the new phenomena we describe. Stimulation could, in principle, occur also for excitons. However, the polariton mass is  $\sim 10^4$  lighter than that for excitons [1]–[4], and, hence, the polariton density of states is very small compared to that for excitons. As a result, it is very much easier to achieve macroscopic state occupancies for polaritons than for excitons, at total densities well below the screening limit where excitons ionize into electron–hole pairs and hence no longer exhibit bosonic properties. As will be discussed in the present paper, specific resonant excitation conditions [6]–[11] facilitate very greatly the efficient popu-

lation of low energy states necessary to achieve large  $N_{final}$ . In recent papers, Butov *et al.* have reported evidence for stimulated scattering for long-lived excitons in type II quantum wells from time-resolved studies [12], and for condensation in local potential minima in spatially resolved studies [13], the long lifetimes enabling exciton cooling to low  $k$  states sufficient to reach high state occupancies.

Most importantly, the unusual shape of the lower polariton dispersion [Fig. 1(b) and (c)] permits new energy and momentum conserving polariton–polariton scattering processes, not possible for either excitons or photons alone [6]–[10]. Such processes can be initiated when resonant excitation is employed close to the point of inflection of the lower polariton (LP) branch, as shown in Fig. 1(c). In this regime, the structure acts like an optical parametric oscillator [8] with efficient conversion of the laser photons into macroscopic populations of two new polariton modes [see Fig. 1(c)]. Such an excitation geometry enables the observation of bosonic stimulation effects and the creation of polariton condensates. In two beam pump–probe geometry, very large ultrafast gains of 100 [6], and subsequently  $\sim 5000$  [14] have been reported for a weak probe beam at  $k = 0$ . The weak probe populates the  $k = 0$  final state and stimulates transitions from the intense pump at the point of inflection to  $k = 0$ , leading to very high gains in the probe beam. Such phenomena form the basis of very high-gain, ultrafast amplifiers with material gains as high as  $10^7 cm^{-1}$  [14].

The paper is organized as follows. The experimental techniques employed for study of polariton effects in microcavities is described in Section II, followed by results for nonres-

onant excitation in Section III. The observation of stimulated scattering for resonant excitation is presented in Section IV, and then the nonresonant and resonant excitation results are compared in Section V, together with a discussion of the potential applicability of such nonresonantly and resonantly excited microcavities as polariton lasers and as high-gain amplifiers and low-threshold oscillators, respectively. Finally, in Section VI, the main points are summarized.

## II. EXPERIMENTAL TECHNIQUES FOR MICROCAVITY STUDIES

Very importantly, the photons and hence the polaritons in a microcavity have a finite lifetime, and therefore their population can be probed directly in well-controlled PL measurements [1]–[4]. Since the in-plane wave vector  $k$  is directly related to the external angle  $\theta$  by  $k = (\omega/c)\sin\theta$ , the distribution of the polariton population can be studied directly in measurements of the PL signal at different angles to the sample normal, as shown in Fig. 1(a). Furthermore, the polaritons can be injected at specific points of the dispersion by varying the angle of incidence of the tunable laser, and the polariton occupation simultaneously probed by varying the detection angle. The one-to-one correspondence between  $k$  and  $\theta$  for the polariton dispersion is a key point in microcavity physics, as opposed to that of polaritons in bulk semiconductors [1]–[4]. Essentially, since the vertical wave vector is quantized in microcavities for both excitons and photons, and as the photons and hence the polaritons have a finite lifetime in the cavity due to leakage through the Bragg mirrors, polaritons can be excited and probed directly in well-controlled experiments. In bulk semiconductors, by contrast, the polaritons are stationary states of the system and can only be converted into external photons by scattering at the sample surface, thus leading to strong distortion of polariton spectra relative to the internal polariton distribution [15].

Most of the experiments described here were carried out under continuous-wave (CW) excitation conditions in cryostats with wide angular access in both excitation and detection channels, with angular resolutions in both cases of  $1^\circ$ . A tunable CW Ti-sapphire laser was used for excitation. The PL was collected by a fiber mounted on a rotating rail and then detected with a high resolution monochromator and nitrogen cooled CCD. Ultrafast experiments in pump-probe geometry, in which a strong pump beam at the point of inflection and a weak probe at  $k = 0$  are employed, are also referred to relatively briefly [6], [9].

## III. NONRESONANT EXCITATION

Photoluminescence spectra excited using CW nonresonant excitation at an energy (1.56 eV) above the stopband of the Bragg mirrors are shown in Fig. 2, for angles of detection from  $0^\circ$  to  $25^\circ$  for two excitation densities of 5 and 80 W/cm<sup>2</sup> (thin and thick lines respectively). The detuning employed is  $-4$  meV. PL signals from both lower and upper polariton branches are observed (the measured dispersions are shown in the inset). Most notably, the signal from the lower polariton branch at 5 W/cm<sup>2</sup> is observed to peak at an angle of  $\sim 20^\circ$  before decreasing to higher angle. This is a signature of the relaxation bottleneck for polaritons, first discussed for bulk

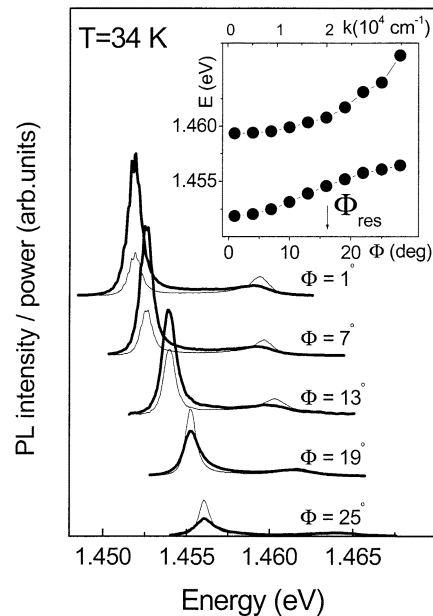


Fig. 2. Angle resolved PL spectra at 34 K for nonresonant excitation at 5 W/cm<sup>2</sup> (thin lines) and 80 W/cm<sup>2</sup> (thick lines). The inset shows the measured polariton dispersion for the detuning of  $-4.3$  meV.

materials (see e.g., [16]), and then for microcavity polaritons by Tassone and co-workers [17], [18], before its definitive observation for III–V [19] and II–VI [20] microcavities respectively. Under the nonresonant excitation conditions employed, the photocreated excitons first relax rapidly by LO phonon relaxation ( $< 1$  ps), followed by slower acoustic phonon emission to populate the high density of high- $k$  exciton states (the exciton reservoir), as indicated schematically in Fig. 1(b). The excitons then relax from the reservoir into the region of strongly coupled polariton states [Fig. 1(b)]. The bottleneck arises as a result of the competition between phonon-assisted polariton relaxation (1-ns timescale) from the exciton reservoir created by the nonresonant excitation, and the increasing escape rate from the cavity as the polariton states become increasingly photon-like with decreasing  $k$ . Furthermore, and again importantly, for the higher power of 80 W/cm<sup>2</sup>, the PL intensity by contrast peaks at  $0^\circ$  and then decreases smoothly to higher angle, showing that the bottleneck is suppressed at higher powers. This result was also confirmed by Senellart *et al.* in [21]. The nonlinear increase of the PL intensity at  $0^\circ$  with power from 5 to 80 W/cm<sup>2</sup> is shown in Fig. 3(a).

These results are summarized in Fig. 3(b), where the PL intensities are plotted as a function of angle (and in-plane  $k$ ). At low power, the PL intensity peaks at  $16^\circ$  and decreases to lower and higher angle. With increasing power, the bottleneck is steadily suppressed as a result of the increasing probability of polariton–exciton and polariton–polariton scattering, until for powers greater than 40 W/cm<sup>2</sup> maximum intensity is observed from  $k = 0$  states. The results in Fig. 3(b) can be converted into relative polariton population  $N_{LP}$  versus  $k$ , since  $N_{LP} \approx I\tau_{LP}$ , where  $\tau_{LP}$  is the time for radiative loss from the cavity given by the photon lifetime in the cavity ( $\sim 1$  ps) divided by the photon fraction of the states involved [Fig. 3(c)]. The resulting polariton populations versus  $k$  are shown in Fig. 4, at temperatures of

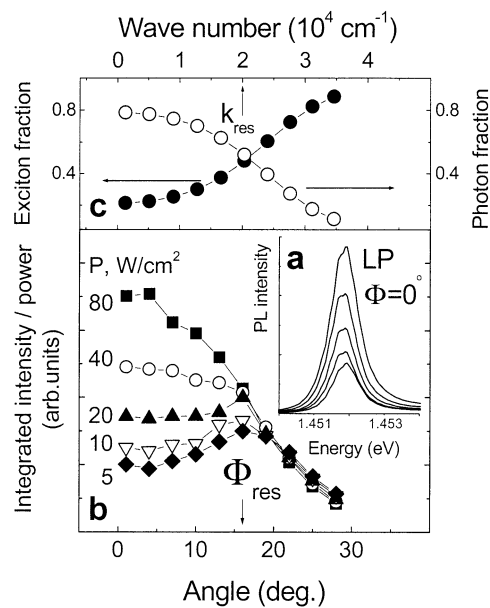


Fig. 3. (a) PL spectra normalized to the laser intensity for  $P$  varying from 5 to 80  $\text{W/cm}^2$ . (b) Integrated LP emission intensity divided by the laser power versus angle for detuning  $\Delta = -4.3$  meV. (c) Photon and exciton fractions of the polariton states for  $\Delta = -4.3$  meV.

1.8 K and 34 K, where the bottleneck at low power and its suppression at high power are clearly seen.

In Fig. 5, angular-dependent PL spectra at low and high power for a range of negative detunings of  $-3$ ,  $-8.7$ , and  $-13.5$  meV are shown, and in Fig. 6, extracted polariton distributions as a function of angle over a wide range of power are presented [22]. It is seen in Fig. 5(a)–(c) that even more pronounced bottlenecks are observed for increasing negative detuning, with  $k = 0$  PL intensities more than one order of magnitude smaller than those at high  $k$  being found at the largest negative detuning. This is a consequence of the very high photon fractions of the low- $k$  states at large detuning and, hence, much reduced relaxation probabilities to low  $k$  before escape occurs from the cavity [the magnitude of the bottleneck defined as the ratio of the  $k = 0$  population to that at high  $k$  is shown as a function of increasing negative detuning in Fig. 4(c)]. Since the microcavities have circular symmetry within the plane of the structures, the observation of PL intensities peaking at finite angle and  $k$  along one line in  $k$  space, as in Fig. 5(a)–(c), corresponds to a ring in the 2-D plane, as observed in recent experiments of Savvidis *et al.* [23]. The variation of population with increasing power for all three detunings is shown in Fig. 6(a)–(c), with in each case the peak of the distribution shifting to smaller  $k$  with increasing power. At  $-3$  meV detuning, the bottleneck is suppressed at relatively low powers of  $\sim 40$   $\text{W/cm}^2$ , and at  $-8.7$  meV it is nearly suppressed at  $\sim 400$   $\text{W/cm}^2$ , whereas at  $-13.5$  meV the peak of the distribution remains at  $20^\circ$ – $25^\circ$ , even at the highest powers studied. It is also notable that the bottleneck is not observed for zero and positive detunings, in contrast to theory predictions [17], [18]. This is probably due to the omission of disorder scattering in the theory treatments, where polariton scattering only by phonons and by excitons or polaritons is included.

Further information on the mechanism responsible for the suppression of the bottleneck with increasing power is obtained

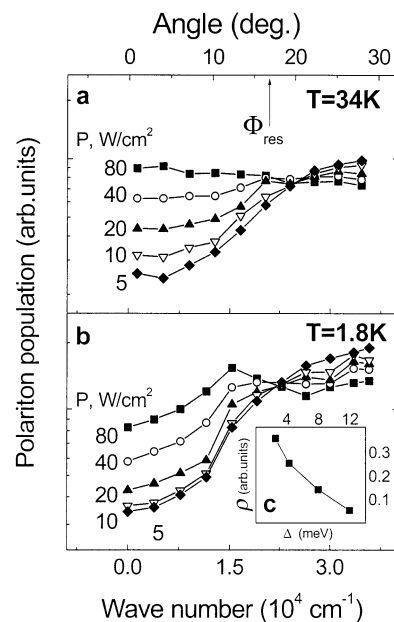


Fig. 4. Polariton population distribution for different excitation densities (a)  $T = 34$  K, (b)  $T = 1.8$  K. (c) Ratio of polariton populations  $\rho = N_{LP}(0)/N_{LP}(k_{\text{res}})$  versus  $\theta$  for low excitation and  $T = 1.8$  K.

from study of the lower polariton branch linewidths as a function of  $k$  at low and high power, as shown in Fig. 7(a)–(c). At low power, the linewidths are approximately independent of angle from  $0^\circ$  to  $35^\circ$ , whereas at 400, 400, and 3200  $\text{W/cm}^2$ , respectively, at the three detunings of Fig. 6, an increase in linewidth by up to a factor of five is observed over this range of angles due to the increased interparticle interaction with increasing density. This is consistent with the accompanying suppression of the bottleneck at similar powers due to polariton–polariton scattering which increasingly populates the low- $k$  states. Further evidence for the role of polariton–exciton scattering in suppressing the bottleneck is also obtained from the greater suppression at a given power with increasing temperature [19], [23], and from the maximum nonlinear behavior in the PL intensity found at an energy of 7 meV below the uncoupled exciton energy, over a wide variety of detunings and temperatures [19].

It is clear from the results of Figs. 3, 4, and 6 that the emission at  $k = 0$  shows marked super-linear increase with increasing laser power [seen clearly in Figs. 3(a) and (b) and 6(a)–(c)]. Further increase of power beyond 400, 800, and 1200  $\text{W/cm}^2$  for the three detunings of Figs. 5 and 6 leads to marked line narrowing and the onset of stimulated emission, as seen in Fig. 5(d)–(f). We showed in [22] that the stimulated emission corresponds to conventional (photon) lasing at the energy of the uncoupled cavity mode, with strong coupling being lost at powers approximately a factor of two below the onset of stimulation. We further demonstrated that the loss of strong coupling occurs when the linewidth at high  $k$  becomes of the order of the Rabi splitting between the modes. Estimates of the exciton density at which strong coupling is lost of  $\sim 7 \times 10^{10} \text{ cm}^{-2}$  are obtained from the experimental laser intensities (see [22]). These values are in good agreement with earlier work by Houdré *et al.* in [24] and theoretical estimates in [25]. Hence, it can be deduced that even though the increasing

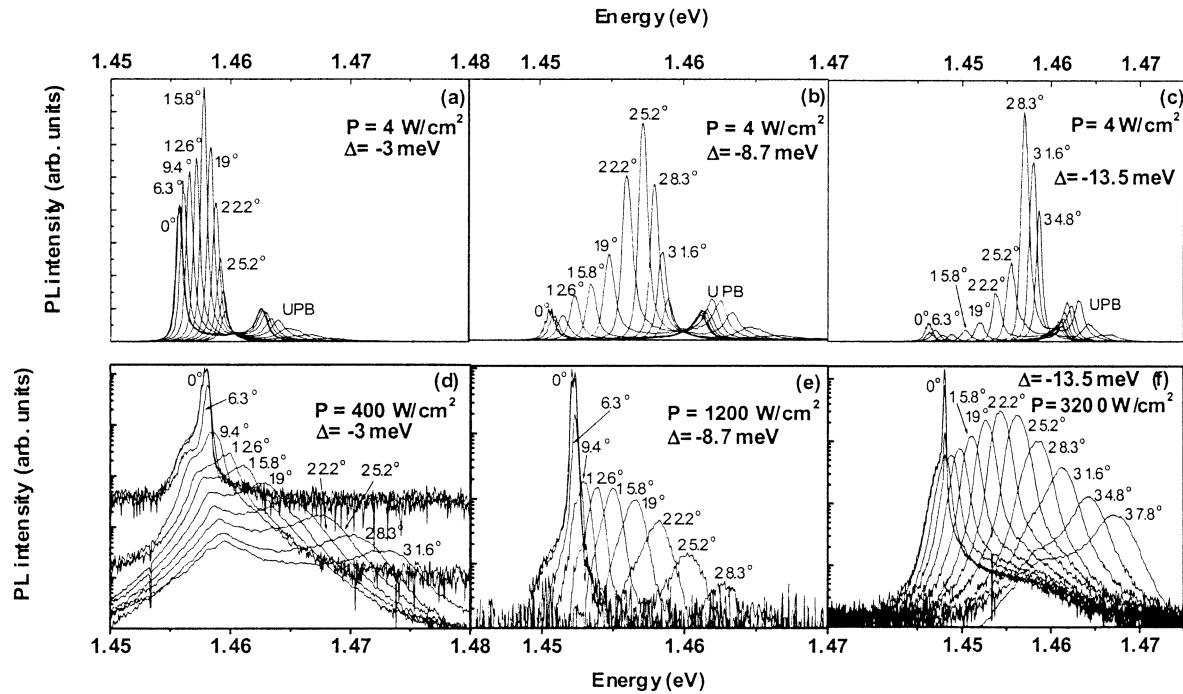


Fig. 5. Angular dependent emission spectra at low powers of  $4 \text{ W/cm}^2$  for  $\Delta = -3, -8.7$  and  $-13.5 \text{ meV}$  in (a)–(c) and above threshold in (d)–(f). Ring emission arising from the relaxation bottleneck is observed at low power, with the maximum in intensity shifting to higher angle with increasing negative detuning. Above threshold the PL shows a sharp stimulated peak at  $\theta = 0$  in each case. At  $\Delta = -3$  and  $-8.7 \text{ meV}$ , the PL decreases in intensity with angle, showing that the bottleneck is suppressed, whereas at  $-13.5 \text{ meV}$ , the PL maximum still occurs at finite angle even in the presence of the stimulation.

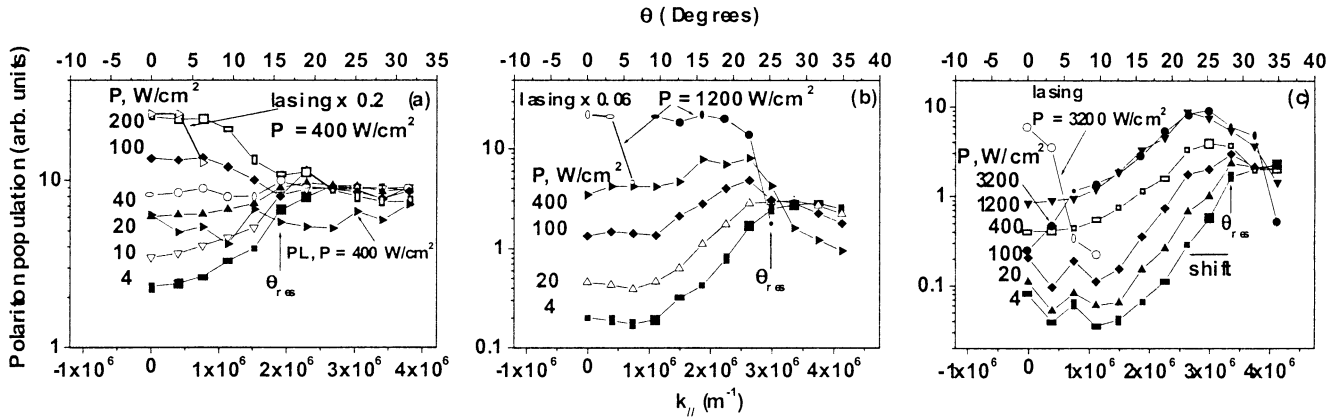


Fig. 6. (a)–(c) Polariton populations, obtained from results of Fig. 4 for  $\Delta = -3, -8.7$  and  $-13.5 \text{ meV}$  as a function of angle (and in-plane wave vector). The bottleneck is suppressed well below threshold in (a), only very close to threshold in (b), whereas in (c) at  $\Delta = -13.5 \text{ meV}$ , the low  $k$  states are still depleted relative to those at high  $k$  even above the stimulation threshold.

exciton–polariton density under conditions of nonresonant excitation leads to increasing population of  $k = 0$  states, at the same time strong population of the exciton reservoir occurs. This leads in turn to increasing exciton broadening, screening, and loss of strong coupling, before polariton occupations greater than one at low  $k$  are achieved, as required to initiate stimulated scattering from the exciton reservoir to  $k = 0$ . The results of [19] and [22], supported by those of [21], show that previous claims [26]–[28] of stimulated polariton scattering (boson behavior [29]), at least in III–V cavities, under conditions of nonresonant excitation were premature.

Very good agreement was obtained between the experimental polariton distributions of Fig. 6(a)–(c) and distributions obtained by numerical solution of the Boltzmann equation

for the photoexcited exciton–polariton system, including exciton–phonon and exciton–exciton scattering terms [22], [30]. The importance of exciton–exciton scattering in overcoming the bottleneck and populating the low- $k$  regions was very clearly demonstrated from the good agreement between experiment and theory. It was furthermore found in the calculations that large exciton populations accumulated in the high- $k$  uncoupled reservoir region, of density sufficient to account for the loss of strong coupling at the highest powers, as observed experimentally. As a result of the good near quantitative agreement with theory, we thus conclude that a good understanding of the polariton distributions and their evolution with excitation density, under conditions of nonresonant excitation, has now been reached.

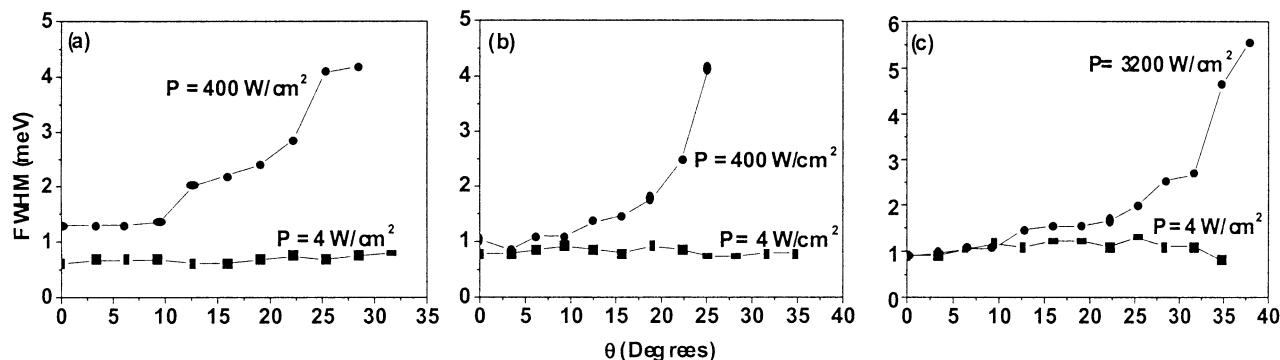


Fig. 7. (a)–(c) Lower polariton branch linewidths (full-width at half-maximum) for  $\Delta = -3, -8.7,$  and  $-13.5$  meV at low power ( $4 \text{ W/cm}^2$ ) and at high power close to or above threshold.

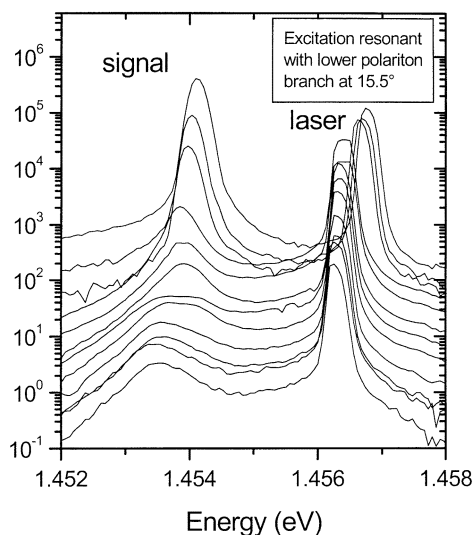


Fig. 8. Photoluminescence spectra at  $\theta = 0^\circ$  for excitation resonant with the lower polariton branch at  $15.5^\circ$ , as a function of excitation intensity from  $0.5 \text{ W/cm}^2$  to  $5 \times 10^2 \text{ W/cm}^2$ . The laser is returned to higher energy to maintain resonance above the threshold of  $\sim 150 \text{ W/cm}^2$  (fifth curve from top).

#### IV. RESONANT EXCITATION

Very different, striking behavior is observed when CW resonant excitation into the lower polariton branch is employed. In this case, polaritons are injected into the polariton region without direct population of the exciton reservoir. Clear evidence for final state stimulation is obtained with the system remaining in the strong coupling regime. Strong line narrowing is found to accompany very strong, superlinear (near exponential) increases in  $k = 0$  intensity, characteristic of a process with gain, stimulated by transitions to a final state with macroscopic occupancy.

The experiments are performed in the geometry shown schematically in Fig. 1(c) and discussed in the introduction. PL spectra detected at  $k = 0$  as a function of laser power for the laser tuned to be in resonance with the point of inflection of the lower polariton branch are shown in Fig. 8(a). The resonant excitation conditions are shown schematically on the  $E-k$  diagram of Figs. 1(c) and 9(b), where it is seen that excitation at  $\sim 16^\circ$  permits pair (parametric) scattering to higher and lower energy in a process conserving energy and momentum.

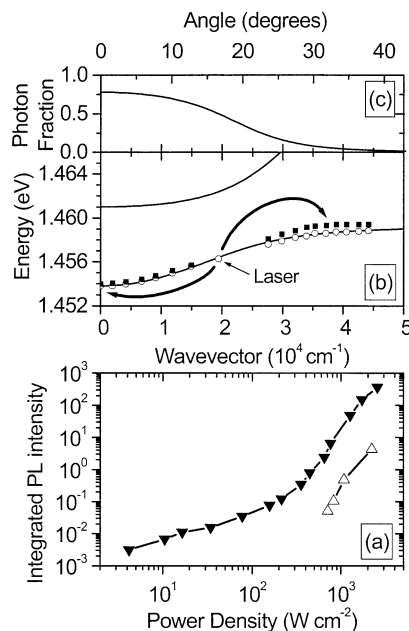


Fig. 9. (a)  $k = 0$  and  $3.9 \times 10^4 \text{ cm}^{-1}$  PL signal intensities versus excitation intensity. Clear threshold behavior is observed at a power density of  $300 \text{ W/cm}^2$ . (b) Measured lower branch dispersions below ( $10 \text{ W/cm}^2$ —open circles) and above threshold ( $300 \text{ W/cm}^2$ —filled squares), together with fitted upper and lower branch dispersions. (c) Calculated photon fraction for lower branch as a function of  $k$ .

This process is described theoretically in [31] and [32]. Strong nonlinear behavior of similar origin, for resonant excitation at an angle of  $10^\circ$ , is reported in [11]. Above a threshold of  $\sim 200 \text{ W/cm}^2$  the spectra show a very marked, near-exponential increase of intensity [see Fig. 8(a)], accompanied by line narrowing to a width of  $0.2$  meV, limited by the spectrometer resolution (subsequent experiments have shown a linewidth of  $0.075$  meV in [10] and as small as  $0.002$  meV in [8]). Accompanying the highly nonlinear increase of intensity [Fig. 9(a)] and the line narrowing, the PL spectra shift by  $0.5$  meV to higher energy and then remain fixed in energy to higher power, so long as the laser energy is also held constant. This behavior is in marked contrast to that observed for nonresonant excitation in Fig. 5(d)–(f), where for each detuning the stimulated peak occurred at the energy of the uncoupled cavity mode, showing that for nonresonant excitation the lasing occurs in the weak coupling limit, as discussed in the previous section.

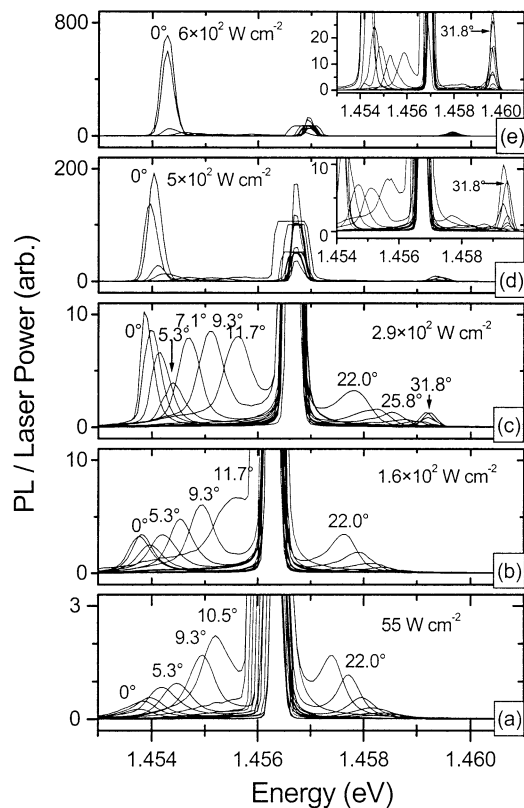


Fig. 10. PL spectra normalized to the laser power for excitation intensities labeled on the figure, (a) below and (b) close to threshold, (c)–(e) above threshold as a function of detection angle from  $0^\circ$  to  $35^\circ$ . A very strong change is observed between (a) at low power where the spectra are strongest for angles close to the excitation energy, and (d), (e) where the spectra are dominated by two peaks at zero and at  $32^\circ$ . The very strong features at  $\sim 1.456$  eV arise from the exciting laser at  $15.5^\circ$ .

The small shift in peak energy from below to above threshold for resonant excitation shows that the highly nonlinear behavior occurs in the strong coupling limit, and strongly suggests the involvement of polariton quasi-particles in the nonlinear process. The blue shift arises from the repulsive polariton–polariton interaction, with the size of the shift determined by the polariton density required to reach threshold [33], [32]. To investigate the behavior further, angular dependent measurements were performed to probe the polariton population distribution as a function of  $k$  for laser powers below, close to, and above threshold, as employed in the nonresonant case in Section III to reveal the existence of the relaxation bottleneck.

The results are shown in Fig. 10. At low power in Fig. 10(a), the PL spectra are seen to peak in intensity around the laser angle and then to decrease in intensity to higher and lower angle [the measured integrated intensities versus  $k$  are shown in Fig. 11(a)]. This is an example of the relaxation bottleneck but now observed for resonantly injected polaritons. At low powers, the polaritons undergo only weak polariton–polariton scattering, leading to small but detectable broadening of the injected population, before escape from the cavity occurs. With increasing power, the polariton distribution broadens further in  $k$  space as the probability for parametric pair scattering increases, until close to threshold in Fig. 10(c), the PL intensity is nearly uniform in  $k$  space for  $k < k_{\text{laser}}$ , with a small peak

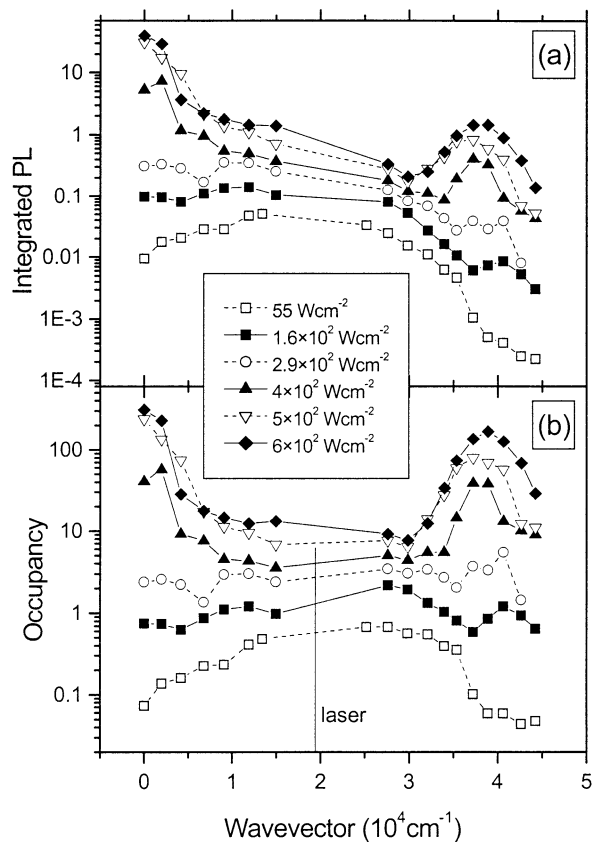


Fig. 11. (a) Integrated intensities of PL peaks as a function of in-plane  $k$  (angle), (b) as (a) but corrected for the photon fraction of the lower branch as a function of  $k$  [from Fig. 9(c)].

developing at  $k = 0$ . Further increase in laser power, now moving above the threshold of Figs. 10 and 11, leads to a very strong increase of the  $k = 0$  intensity, accompanied by an additional strong peak at high  $k$ . This is the high  $k$  component of the pair scattering process indicated schematically in Fig. 9(b), required to conserve energy and momentum in the process  $2k_{\text{laser}} = k_{\text{signal}} + k_{\text{idler}}$ ,  $2E_{\text{laser}} = E_{\text{signal}} + E_{\text{idler}}$ , where the subscripts signal and idler refer to the  $k = 0$  and high  $k$  beams, respectively. Furthermore, measurements of the polariton dispersion above threshold show that the polariton dispersion curve is only slightly modified from the case at low power [Fig. 9(b)] and that the system remains clearly in the strong coupling limit. The angular dependent measurements thus show that the strong nonlinear behavior observed for resonant excitation has a very different origin than that for nonresonant excitation, and that it arises from a polariton–polariton scattering process in the strong coupling regime to states at  $k = 0$  and high  $k$ , as discussed further below.

The final step in elucidating the physics underlying the results of Figs. 8–11 was to convert the PL intensities versus  $k$  of Fig. 11(a) to polariton populations versus  $k$ . First, the relative PL intensities are converted to relative polariton occupancies by correcting the observed PL intensities by the photon fraction (and hence lifetime) of the states involved [Fig. 9(c)]. Carrying out this correction leads to polariton occupancies in the signal and idler states within a factor of two of one another, as shown in Fig. 11(b), consistent with the pair nature of the

process which gives rise to the two beams. Finally, measurement of the absolute power ( $P$ ) emitted in the  $k = 0$  beam enables the occupancies ( $N$ ) to be placed on an absolute scale since  $N = (I_{\text{PL}}\tau_{\text{pol}}4\pi)/(\Delta k)^2$ , where  $I_{\text{PL}}$  is the measured PL power in watts,  $\tau_{\text{pol}}$  is the polariton lifetime given by the photon lifetime in the cavity divided by the photon fraction of the  $k = 0$  state and  $\Delta k$  is the width in  $k$  space of the  $k = 0$  beam. Carrying out this procedure shows that the occupancy of the  $k = 0$  state at threshold is equal to unity within a total error of a factor of  $\pm 3$  [6]. This is exactly the condition discussed in the introduction necessary for the occurrence of final state stimulation of the pair-scattering process. Taken together with the proof from the spectra and the dispersion above threshold that the signal beam arises from a system in the strong coupling limit, this result provides strong evidence for the occurrence of final state stimulation arising from the bosonic character of the polariton quasi-particles.

The scattering process to two specific points in  $k$  space has some of the characteristics of a polariton condensation, to a final state with large occupancy, with the state occupancy reaching values greater than 100 at the highest powers employed. Furthermore, the strong line narrowing shows that the final state has macroscopic coherence. The spontaneous appearance of line narrowing above threshold shows that the polariton system has undergone a phase transition, consisting of the macroscopic occupation of a single mode. Since polaritons are bosons, there is some justification in describing this phase as a Bose–Einstein condensate (BEC). Support for this description is provided by clear observation of stimulated scattering of other polaritons into the macroscopically occupied mode, a characteristic property of a BEC. However, the system is far from thermal equilibrium, so although the initial build-up of the  $k = 0$  population comes from scattering down from the pump population, the phase transition is not driven by cooling of the system. In this sense, the phenomena differs from the ideal picture of a BEC, which has a well-defined temperature and a chemical potential approaching zero.

Stimulated scattering was first reported in two beam ultrafast pump–probe experiments [6]. In this case, a strong pump beam is incident on the sample at the point of inflection of the lower polariton branch. Very weak scattering to  $k = 0$  was found with the pump beam alone present on the sample, probably because only a very small  $k = 0$  population builds up before the pump pulse ends and the photogenerated polaritons escape from the sample. Injection of a weak probe at  $k = 0$  was found to lead to very strong stimulated scattering from  $k_{\text{laser}}$  to  $k = 0$  with very large gains of order 100 being found. In the CW excitation experiments, by contrast the process is self-stimulated, with sufficient  $k = 0$  population building up to lead to strong stimulation without the need for injection of a second probe pulse. Erland *et al.* have subsequently observed stimulation in ultrafast measurements in the presence of the pump alone on very high quality samples with photon lifetimes of  $\sim 10$  ps [34].

Subsequent pump–probe measurements on higher quality samples have reported probe gains up to 5000 [14], demonstrating the potential of microcavities as very high gain, ultrafast amplifiers (the duration of the gain is given by a combination of pulse durations and the polariton lifetimes in the cavity, all

having picosecond timescales). This work reported amplification up to temperatures of 220 K, the upper temperature limit being shown to originate from exciton ionization and, hence, loss of strong coupling (we return to this point in Section V from the device point of view).

The stimulated scattering behavior has a number of similarities to four-wave mixing and optical parametric amplifier and oscillator (OPO). The phenomena reported in [7] and [8] correspond to conversion efficiencies from pump absorbed to signal of  $\sim 10\%$ , at thresholds many orders of magnitude less than in conventional OPOs, the low threshold arising as a result of the triply resonant nature of the process, with laser, signal, and pump all resonant with points on the dispersion curve. Indeed, theoretical descriptions of the behavior have been published based either on a purely classical nonlinear treatment [32] or a quantum bosonic picture [33], but using nonlinear equations familiar from treatments of OPOs. However, it should be realized that the distinction between a description of the phenomena in terms of stimulated scattering of bosonic quasi-particles and a parametric oscillator description in terms of triply resonant nonlinear optical behavior, is mainly one of nomenclature only ([33] uses the equations of the parametric amplifier and oscillator but with quantization of the polariton field).

Within the framework of nonlinear optics, the behavior under resonant excitation can be understood as an unusual type of optical parametric oscillator [32]. It is unusual because it occurs in the strong coupling regime, and because the nonlinearity is a resonant  $\chi_3$  effect, with two pump polaritons scattering into the signal and idler modes. This contrasts with the normal nonresonant  $\chi_2$  OPO, where a single pump photon splits into a signal and an idler of roughly half the energy. However, the behavior expected and observed in the microcavity has many similarities to that of the normal  $\chi_2$  OPO: as the pump power is increased from zero, there is a threshold beyond which a coherent occupation of signal and idler modes develops. This corresponds to the power at which the scattering into the signal and idler modes from the pump is strong enough to overcome the losses from those modes. The losses include emission as external photons, and transfer into the high momentum reservoir states, due to disorder scattering, and at higher intensities in CW experiments, exciton–polariton scattering [35]. Thus, threshold rises in disordered samples and at high intensities. Above the threshold, the signal intensity is proportional to the square root of the pump power, and the population of the pump mode remains constant, with all the additional pump power transferred into the signal and idler modes. The  $\chi_3$  nonlinearity also provides an explanation for the blue shift observed in microcavity dispersion measurements, which does not occur for a normal  $\chi_2$  OPO. It arises from the repulsive interaction of polaritons at different points on the dispersion with the coherent pump population. In a scattering picture, this corresponds to, for example, signal and pump polaritons scattering off each other but remaining in the same modes. Provided there is only one significant coherent population in the system (the pump mode), the blue shift provides a convenient measure of this population. Below the threshold, the blueshift of the dispersion increases linearly with pump power, as the pump population grows, but above the shift remains constant, because the pump population is locked at its threshold

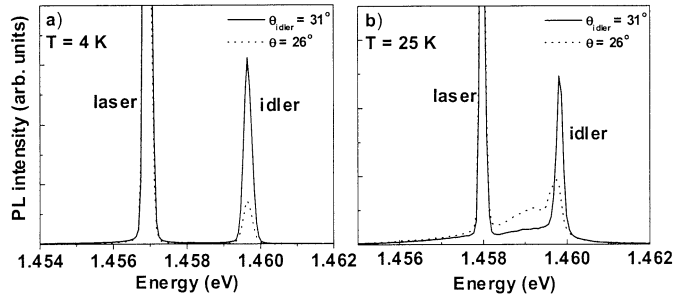


Fig. 12. Comparison of idler spectra at temperatures of (a) 4 K and (b) 25 K, measured at the peak of the idler at  $31^\circ$ , and at an angle of  $26^\circ$ . The strong decrease of the idler relative to background PL at higher temperature is clearly seen.

value. The value above threshold is independent of the strength of the nonlinearity, and depends only on the exciton fractions and linewidths of the signal and idler modes.

We stress that the evidence for the involvement of real polariton quasi-particles in the scattering phenomena is strong. This is demonstrated, for example, by the strong modifications in the polariton distribution from below to above threshold in Figs. 10 and 11, and the strong temperature dependence of the idler signal shown in Fig. 12, where it is seen that the idler is strongly suppressed with increasing temperature, due to the increasing probability of elastic scattering to the exciton reservoir at elevated temperature. Such behavior finds a natural explanation on the basis of the creation of real quasi-particles at the idler  $k$ .

Further interesting phenomena involving the occurrence of higher order polariton scattering processes, when the laser signal and idler modes are macroscopically occupied, are observed in both ultrafast [36] and CW [37] measurements. Additional stimulated peaks at  $3k_{\text{laser}}$  and  $-k_{\text{laser}}$  are observed at energies and wave vectors lying off both the unperturbed or renormalized dispersion curves, as shown in Figs. 13 and 14—observations which find a natural explanation within the quantum bosonic description of the observed phenomena [36], [38].

#### V. COMPARISON OF RESONANT AND NONRESONANT EXCITATION OF MICROCAVITIES, POLARITON LASERS, AND OPTICAL PARAMETRIC OSCILLATORS

The discussions in Sections III and IV show that carrier-carrier (pair) scattering processes (exciton-exciton, exciton-polariton and polariton-polariton) play a determining role in the polariton distributions which result from both nonresonant and resonant excitation of semiconductor microcavities.

In the nonresonant case at  $\sim -3$  meV negative detuning, suppression of the bottleneck by polariton-polariton scattering is observed for power densities of  $\sim 40$  W/cm<sup>2</sup>, with further increase of power to  $\sim 400$  W/cm<sup>2</sup> leading to lasing in the weak coupling limit. The strong coupling is lost due to exciton screening at carrier densities estimated to be  $\sim 4 \times 10^{11}$  cm<sup>-2</sup> (assuming an exciton lifetime of 0.5 ns), corresponding to an exciton density per well of  $7 \times 10^{10}$  cm<sup>-2</sup> [24], close to the Mott limit for excitons in quantum wells. Further clear evidence for the importance of exciton-exciton interactions

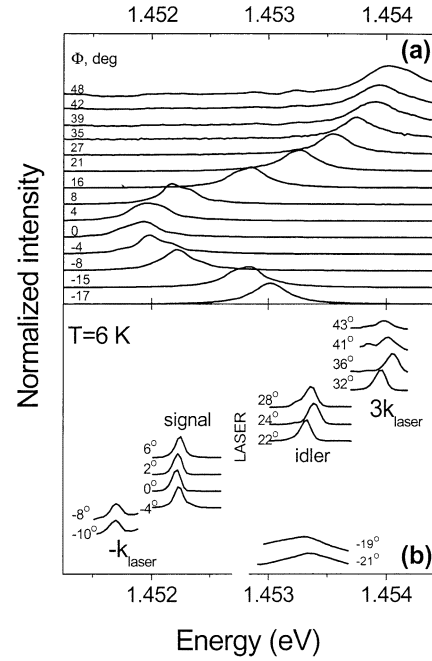


Fig. 13. (a) Angle resolved PL spectra for the lower polariton branch for low intensity illumination into the upper polariton branch. (b) As (a) but above threshold for resonant excitation close to the point of inflection of the lower polariton branch. Strong stimulated peaks at  $k_{\text{signal}}$ ,  $-k_{\text{laser}}$ ,  $k_{\text{idler}} (=2k_{\text{signal}})$  and  $3k_{\text{laser}}$  are observed.

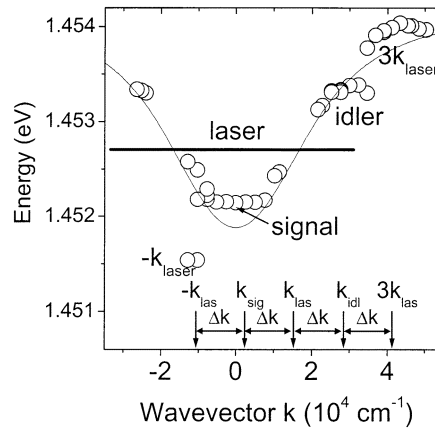


Fig. 14. Dispersions of the stimulated peaks at  $k_{\text{signal}}$ ,  $-k_{\text{laser}}$ ,  $k_{\text{idler}} (=2k_{\text{signal}})$  and  $3k_{\text{laser}}$  peaks, together with the dispersion below threshold (full line). The  $-k_{\text{laser}}$ , and  $3k_{\text{laser}}$  arise from scattering processes involving the macroscopically occupied signal and idler states, to states off the unperturbed polariton branches.

was obtained from the marked increase of polariton linewidth for angles greater than  $\sim 16^\circ$  in Fig. 7. However, polariton final stimulation plays no role in the observed behavior, with strong coupling being lost before  $k = 0$  occupancies become sufficiently large (greater than one) to initiate stimulation. The main difficulty with nonresonant excitation is that most of the photocreated carriers relax into the exciton reservoir with inefficient population of the small  $k$  polariton states. Attempts to increase the low  $k$  polariton population up to state occupancies close to unity leads to population of the exciton reservoir at densities greater than the exciton screening limit, with loss of strong coupling before stimulation occurs [22].

The case of resonant excitation is very different. In this case, polaritons are injected into the polariton region without direct population of the exciton reservoir. Polariton–polariton scattering leads to population of states at lower and higher  $k$ . Stimulation is observed at incident power densities of  $\sim 200$  W/cm<sup>2</sup>, corresponding to a parametric process to pair states at  $k = 0$  and high  $k$ . Most importantly, the lifetime of the injected particles is now given by the polariton lifetime (close to the photon lifetime of  $\sim 1$  ps), and the threshold is now achieved at a polariton density of only  $\sim 10^8$  cm<sup>-2</sup>, well below the density for any significant screening. Hence, the strong coupling limit is retained at  $k = 0$  state occupancies in excess of unity, as shown in Section IV, permitting the occurrence of polariton final state stimulation; stimulated scattering of the bosonic polariton particles to the  $k = 0$  states is achieved while remaining firmly in the strong coupling regime. The polariton state has macroscopic coherence, as indicated by its very narrow linewidth, and emits photons at a rate controlled by the photon lifetime in the cavity, determined by the finesse of the Fabry–Pérot cavity.

The achievement of stimulated scattering from the exciton reservoir to  $k = 0$  under conditions of nonresonant excitation followed by photon escape has the potential to lead to a new form of light source, originally discussed for bulk semiconductors by Keldysh [39] and subsequently for microcavities by Imamoglu and Ram [29]. The stimulated scattering leads to the formation of a state with macroscopic coherence at  $k = 0$ , which subsequently emits as a source of coherent photons, termed the “polariton laser.” Such a source is in marked contrast to a conventional laser where the photon emission process itself is stimulated, leading to macroscopic occupation of particular photon modes of the cavity.

In order to achieve polariton lasing under conditions of nonresonant excitation, it is necessary that  $k = 0$  occupancies greater than one be achieved before the strong coupling is lost due to exciton screening from the high density of excitons inevitably created in the exciton reservoir. However, if the strong coupling were retained, the stimulation mechanism would then lead to very efficient scattering from the reservoir down to  $k = 0$ , and thus very efficient population of the emitting states. Such a mechanism would form the basis of a new light source where injected carriers populate the “lasing” state on an ultrafast timescale. The results presented in Section III show that such a situation cannot be achieved in GaAs-based III–V microcavities, due largely to the relatively small exciton binding energies ( $\sim 8$  meV) and correspondingly low densities for exciton screening. However, it has recently been shown theoretically that the introduction of electrons into the quantum wells at densities of order  $10^{10}$  cm<sup>-2</sup>, well below the screening limit, will lead to much more effective population of the low- $k$  states [30]. This arises both from the much larger exciton–electron scattering cross section than for exciton–exciton scattering, and from the small electron mass, four to five times smaller than for excitons, which makes large polariton energy loss  $k = 0$  loss significantly more probable.

II–VI [40], GaN [41], and organic [42] microcavities all offer potentially more favorable systems for the achievement of polariton stimulation under nonresonant conditions, due to their significantly greater exciton binding energies (factors of three

to ten higher in the sequence II–VI, GaN, organic) and exciton oscillator strengths. The larger exciton binding energies provide much greater resistance to screening than the GaAs-based structures. Furthermore, the large binding and large Rabi splittings will permit study at temperatures in the range 100 K–300 K without the loss of strong coupling, thus increasing the probability for the required energy and wave vector conserving scattering out of the reservoir to low  $k$  states [18], [23]. It should be noted that relatively early experiments on II–VI microcavities did provide possible evidence for polariton lasing at intermediate excitation densities [40], before collapse of the system to the weak coupling regime at higher powers, thus giving optimism that such a polariton laser can be achieved in systems with large exciton binding energy. Indeed, model calculations for GaN microcavities, with very large Rabi splitting of 90 meV [41], predict the occurrence of stimulated scattering to  $k = 0$  without the onset of screening. It should also be noted that the observation of “polariton lasing” would correspond to the formation of a nonequilibrium Bose condensate by stimulated scattering from the high-energy exciton reservoir, a significant achievement from the fundamental point of view. In this context, recent work in [43] reporting stimulation to states of finite  $k$  under nonresonant excitation of a II–VI cavity is also noteworthy.

The resonantly excited microcavities also have considerable potential as highly efficient, triply resonant optical parametric oscillators (OPOs) [8], [7] and ultrafast high-gain amplifiers [6], [14], as discussed in Section III. For these applications, structures with large polariton branch splittings and high exciton binding energies are also likely to be highly advantageous. Impressive results have already been obtained with amplifier gains up to 5000 at low temperature [14], gain up to temperatures of  $\sim 220$  K [14], and CW oscillator conversion efficiencies of  $\sim 10\%$  [7], all achieved in very compact micrometer scale devices, in strong contrast to the many orders of magnitude higher power densities and millimeter to centimeter crystal sizes in conventional OPAs or OPOs. Progress is now likely toward room temperature operation in wide-bandgap, high-oscillator strength, high binding energy materials, which permit the necessary exciton and polariton stability up to 300 K and above. Such efforts are now underway in a number of laboratories worldwide. A further advantage of the high oscillator strength materials is that the large Rabi splittings will in turn give rise to large energy splittings between pump, signal and idler and, hence, the desirable large wavelength shifts in OPO applications.

## VI. SUMMARY

Recently discovered phenomena that arise from the bosonic character of the polariton quasi-particles in semiconductor microcavities have been described. Typical bosonic phenomena such as stimulated scattering by final state occupation and macroscopic occupation of states are observed. The key features of microcavities which lead to these observations, including finite energy at  $k = 0$ , very small density of states, and dispersions which permit new quasi-particle scattering processes, have been emphasized. The strong contrast between phenomena observed under nonresonant and resonant

excitation conditions have been emphasized. Prospects for the creation of polariton lasers, and high gain, triply resonant ultrafast amplifiers and very low threshold optical parametric oscillators have been discussed.

#### ACKNOWLEDGMENT

The authors express their great thanks to J. J. Baumberg for their long standing collaboration in the field of microcavities which has been fundamental to the success of much of this work. They also acknowledge gratefully the interactions with P. G. Savvidis, V. D. Kulakovskii, D. N. Krizhanovskii, G. Malpuech and A. V. Kavokin, and to J. S. Roberts who grew the high quality samples without which this work could not have taken place.

#### REFERENCES

- [1] M. S. Skolnick, T. A. Fisher, and D. M. Whittaker, "Strong coupling phenomena in quantum microcavity structures," *Semicond. Sci. Technol.*, vol. 13, pp. 645–669, 1998.
- [2] G. Khitrova, H. M. Gibbs, F. Jahnke, M. Kira, and S. W. Koch, "Non-linear optics of normal-mode-coupling semiconductor microcavities," *Rev. Mod. Phys.*, vol. 71, pp. 1591–1639, 1999.
- [3] M. S. Skolnick, R. M. Stevenson, A. I. Tartakovskii, R. Butté, M. Emam-Ismaïl, D. M. Whittaker, P. G. Savvidis, J. J. Baumberg, A. Lemaître, V. N. Astratov, and J. S. Roberts, "Polariton–polariton interactions and stimulated scattering in semiconductor microcavities," *Mater. Sci. Eng.*, vol. C19, pp. 407–415, 2002.
- [4] A. I. Tartakovskii, M. S. Skolnick, D. N. Krizhanovskii, V. D. Kulakovskii, R. M. Stevenson, R. Butté, J. J. Baumberg, D. M. Whittaker, and J. S. Roberts, "Stimulated polariton scattering in semiconductor microcavities: New physics and potential applications," *Adv. Mater.*, vol. 13, pp. 1725–1731, 2001.
- [5] C. Weisbuch, M. Nishioka, A. Ishikawa, and Y. Arakawa, "Observation of the coupled exciton–photon mode splitting in a semiconductor quantum microcavity," *Phys. Rev. Lett.*, vol. 69, pp. 3314–3417, 1992.
- [6] P. G. Savvidis, J. J. Baumberg, R. M. Stevenson, M. S. Skolnick, D. M. Whittaker, and J. S. Roberts, "Angle resonant stimulated polariton amplifier," *Phys. Rev. Lett.*, vol. 84, pp. 1547–1550, 2000.
- [7] R. M. Stevenson, V. N. Astratov, M. S. Skolnick, M. Emam-Ismaïl, D. M. Whittaker, A. I. Tartakovskii, P. G. Savvidis, J. J. Baumberg, and J. S. Roberts, "Continuous wave observation of massive polariton redistribution by stimulated scattering in semiconductor microcavities," *Phys. Rev. Lett.*, vol. 85, pp. 3680–3683, 2000.
- [8] J. J. Baumberg, P. G. Savvidis, R. M. Stevenson, A. I. Tartakovskii, M. S. Skolnick, D. M. Whittaker, and J. S. Roberts, "Parametric oscillation in a vertical microcavity: a polariton condensate or micro-optical parametric oscillation," *Phys. Rev.*, vol. B62, pp. R16 247–16 250, 2000.
- [9] P. G. Savvidis, J. J. Baumberg, R. M. Stevenson, M. S. Skolnick, D. M. Whittaker, and J. S. Roberts, "Asymmetric angular emission in semiconductor microcavities," *Phys. Rev.*, vol. B62, pp. R13 278–13 281, 2000.
- [10] A. I. Tartakovskii, D. N. Krizhanovskii, and V. D. Kulakovskii, "Polariton–polariton scattering in semiconductor microcavities: Distinctive features and similarities to the three-dimensional case," *Phys. Rev.*, vol. B62, pp. R13 298–13 301, 2000.
- [11] R. Houdré, C. Weisbuch, R. P. Stanley, U. Oesterle, and M. Ilegems, "Nonlinear emission of semiconductor microcavities in the strong coupling regime," *Phys. Rev. Lett.*, vol. 85, pp. 2793–2796, 2000.
- [12] L. V. Butov, A. L. Ivanov, A. Imamoglu, P. B. Littlewood, A. A. Shashkin, V. T. Dolgoplov, K. L. Campman, and A. C. Gossard, "Stimulated scattering of indirect excitons in coupled quantum wells: Signature of a degenerate Bose-gas of excitons," *Phys. Rev. Lett.*, vol. 86, pp. 5608–5611, 2001.
- [13] L. V. Butov, C. W. Lai, A. L. Ivanov, A. C. Gossard, and D. S. Chemla, "Towards Bose–Einstein condensation of excitons in potential traps," *Nature*, vol. 417, pp. 47–50, 2002.
- [14] M. Saba, C. Ciuti, J. Bloch, V. Thierry-Mieg, R. André, L. S. Dang, S. Kundermann, A. Mura, G. Bongiovanni, J. L. Staehli, and B. Deveaud, "High-temperature ultrafast polariton parametric amplification in semiconductor microcavities," *Nature*, vol. 414, pp. 731–734, 2001.
- [15] E. Koteles, *Excitons*, E. I. Rashba and M. D. Sturge, Eds. Amsterdam, The Netherlands: North Holland, 1982, p. 85.
- [16] J. Toyozawa, *Suppl. Prog. Theor. Phys.*, vol. 12, pp. 11–20, 1959.
- [17] F. Tassone, C. Piermarocchi, V. Savona, A. Quattropani, and P. Schwendimann, "Bottleneck effects in the relaxation and photoluminescence of microcavity polaritons," *Phys. Rev.*, vol. B56, pp. 7554–7557, 1997.
- [18] F. Tassone and Y. Yamamoto, "Exciton–exciton scattering dynamics in a semiconductor microcavity and stimulated scattering into polaritons," *Phys. Rev.*, vol. B59, pp. 10 830–10 836, 1999.
- [19] A. I. Tartakovskii, M. Emam-Ismaïl, R. M. Stevenson, M. S. Skolnick, V. N. Astratov, D. M. Whittaker, J. J. Baumberg, and J. S. Roberts, "Relaxation bottleneck and its suppression in a semiconductor microcavity," *Phys. Rev.*, vol. B62, pp. R2283–2286, 2000.
- [20] M. Müller, J. Bleuse, and R. André, "Dynamics of the cavity polariton in CdTe-based semiconductor microcavities: Evidence for a relaxation edge," *Phys. Rev.*, vol. B62, pp. 16 886–16 890, 2000.
- [21] P. Senellart, J. Bloch, B. Sermage, and J. Y. Marzin, "Microcavity polariton depopulation as evidence for stimulated scattering," *Phys. Rev.*, vol. B62, pp. R16 263–16 266, 2000.
- [22] R. Butté, G. Delalleau, A. I. Tartakovskii, M. S. Skolnick, V. N. Astratov, J. J. Baumberg, G. Malpuech, A. DiCarlo, A. V. Kavokin, and J. S. Roberts, "Transition from strong to weak coupling and the onset of lasing in semiconductor microcavities," *Phys. Rev.*, vol. B65, pp. 205 310–205 316, 2002.
- [23] P. G. Savvidis, J. J. Baumberg, D. Porras, D. M. Whittaker, M. S. Skolnick, and J. S. Roberts, "Ring emission and exciton-pair scattering in semiconductor microcavities," *Phys. Rev.*, vol. B65, pp. 073 309–073 312, 2002.
- [24] R. Houdré, J. L. Gibernon, P. Pellandini, R. P. Stanley, U. Oesterle, C. Weisbuch, J. O’Gorman, B. Roycroft, and M. Ilegems, "Saturation of the strong-coupling regime in a semiconductor microcavity: Free-carrier bleaching of cavity polaritons," *Phys. Rev.*, vol. B52, pp. 7810–7813, 1995.
- [25] M. Kira, F. Jahnke, S. W. Koch, J. D. Berger, D. V. Wick, T. R. Nelson, G. Khitrova, and H. M. Gibbs, "Quantum theory of nonlinear semiconductor microcavity luminescence explaining 'Boser' experiments," *Phys. Rev. Lett.*, vol. 79, pp. 5170–5173, 1997.
- [26] P. Senellart and J. Bloch, "Nonlinear emission of microcavity polaritons in the low density regime," *Phys. Rev. Lett.*, vol. 82, pp. 1233–1236, 1999.
- [27] S. Pau, H. Cao, J. Jacobson, G. Björk, and Y. Yamamoto, "Observation of a laserlike transition in a microcavity exciton polariton system," *Phys. Rev.*, vol. A54, pp. R1789–1792, 1996.
- [28] H. Cao *et al.*, "Transition from a microcavity exciton polariton to a photon laser," *Phys. Rev.*, vol. A55, pp. 4632–4635, 1997.
- [29] A. Imamoglu and R. J. Ram, "Quantum dynamics of exciton lasers," *Phys. Lett.*, vol. A214, pp. 193–197, 1996.
- [30] G. Malpuech, A. V. Kavokin, A. Di Carlo, and J. J. Baumberg, "Polariton lasing by exciton–electron scattering in semiconductor microcavities," *Phys. Rev.*, vol. B65, pp. 153 310–153 313, 2002.
- [31] C. Ciuti, P. Schwendimann, and A. Quattropani, "Parametric luminescence of microcavity polaritons," *Phys. Rev.*, vol. B63, pp. R041 303–041 306, 2001.
- [32] D. M. Whittaker, "Classical treatment of parametric processes in a strong-coupling planar microcavity," *Phys. Rev.*, vol. B63, pp. 193 305–193 308, 2001.
- [33] C. Ciuti, P. Schwendimann, B. Deveaud, and A. Quattropani, "Theory of the angle-resonant polariton amplifier," *Phys. Rev.*, vol. B62, pp. R4825–4828, 2000.
- [34] J. Erland, V. Mizeikis, W. Langbein, J. R. Jensen, and J. M. Hvam, "Stimulated secondary emission from semiconductor microcavities," *Phys. Rev. Lett.*, vol. 86, pp. 5791–5794, 2001.
- [35] A. I. Tartakovskii, D. N. Krizhanovskii, D. A. Kurysh, V. D. Kulakovskii, M. S. Skolnick, and J. S. Roberts, "Threshold power and internal loss in the stimulated scattering of microcavity polaritons," *Phys. Rev.*, vol. B66, pp. 165 329–165 332, 2002.
- [36] P. G. Savvidis, C. Ciuti, J. J. Baumberg, D. M. Whittaker, M. S. Skolnick, and J. S. Roberts, "Off branch polaritons and multiple scattering in semiconductor microcavities," *Phys. Rev.*, vol. B64, pp. 075 311–075 314, 2001.
- [37] A. I. Tartakovskii, D. N. Krizhanovskii, D. A. Kurysh, V. D. Kulakovskii, M. S. Skolnick, and J. S. Roberts, "Polariton parametric scattering processes in semiconductor microcavities observed in continuous wave experiments," *Phys. Rev.*, vol. B65, pp. 081 308–081 311, 2002.
- [38] S. A. Moskalenko and D. W. Snoke, *Bose–Einstein Condensation of Excitons and Biexcitons and Coherent Non-Linear Optics With Excitons*. Cambridge, U.K.: Cambridge Univ. Press, 2000, p. 275.

- [39] L. V. Keldysh, *Bose-Einstein Condensation*, A. Griffin, D. W. Snoke, and S. Stringari, Eds. Cambridge, U.K.: Cambridge Univ. Press, 1995, p. 256.
- [40] L. S. Dang, D. Heger, R. André, F. Boeuf, and R. Romestain, "Stimulation of polariton photoluminescence in semiconductor microcavity," *Phys. Rev. Lett.*, vol. 81, pp. 3920–3923, 1998.
- [41] G. Malpuech, A. di Carlo, A. V. Kavokin, J. J. Baumberg, A. Zamfirescu, and P. Lugli, "Room-temperature polariton lasers based on GaN microcavities," *Appl. Phys. Lett.*, vol. 81, pp. 412–414, 2002.
- [42] D. G. Lidzey, D. D. C. Bradley, T. Virgili, A. Armitage, M. S. Skolnick, and S. Walker, "Room temperature polariton emission from strongly coupled organic semiconductor microcavities," *Phys. Rev. Lett.*, vol. 82, pp. 3316–3619, 1999.
- [43] R. Huang, Y. Yamamoto, R. André, J. Bleuse, M. Müller, and H. Ulmer-Tuffigo, "Exciton-polariton lasing and amplification based on exciton-exciton scattering in CdTe microcavity quantum wells," *Phys. Rev.*, vol. B65, pp. 165 315–165 318, 2002.



**M. S. Skolnick** received the Ph.D. degree from the University of Oxford, Oxford, U.K., in 1975.

He spent two years as a postdoctoral worker at the Max-Planck-Institute, Grenoble, France. He then moved to the Royal Signals and Radar Establishment, Malvern, U.K., in 1978, where he spent the next 13 years, in the last three years as a Senior Principal Scientific Officer (individual merit). In January 1991, he was appointed as Professor of Condensed Matter Physics at the University of Sheffield, Sheffield, U.K. In addition to leading his own research group, he is Deputy Director of the EPSRC Central Facility for III–V Materials, the national U.K. center for the fabrication of III–V semiconductor structures. His principal research interests include the study of the optoelectronic properties of semiconductor low-dimensional structures, particularly quantum dots, photonic structures with emphasis on control of light matter interactions, and the investigation of new midinfrared light sources.

Dr. Skolnick was awarded an EPSRC Senior Research Fellowship in 2001 and received the Mott Medal and Prize of the Institute of Physics in 2002.

**Alexander I. Tartakovskii** was born in Astrakhan, Russia, on December 27, 1973. He received his diploma in physics and applied math from Moscow Institute of Physics and Technology (MIPT), Moscow, Russia, in 1996 and the Ph.D. degree from the Institute of Solid State Physics, Chernogolovka, Russia, in 1998.

In 1993, during his studies in MIPT, he started his work at the Institute of Solid State Physics. In 2001, he moved to the University of Sheffield, Sheffield, U.K. During the past eight years, he was actively involved into numerous experiments on optics of semiconductor heterostructures with a particular emphasis on nonlinear effects.



**Raphaël Butté** received the Ph.D. degree from the Université Claude Bernard of Lyon, France, in 2000. His thesis was on structural and optoelectronic properties of hydrogenated polymorphous silicon, an heterogeneous semiconductor close to hydrogenated amorphous silicon.

Since 2000, he has been a Postdoctoral Research Associate at the University of Sheffield, Sheffield, U.K., in the group of Prof. M. S. Skolnick. His current research interest deals with the study of III–V semiconductor microcavities in the strong coupling regime and more precisely condensation phenomena of polaritons in semiconductor microcavities. He is the co-author of 14 publications and one book chapter.

**D. M. Whittaker**, photograph and biography not available at the time of publication.



**R. Mark Stevenson** received the first class degree in pure and applied physics from the University of Nottingham, Nottingham, U.K., in 1997.

He joined the group led by M. S. Skolnick at the University of Sheffield, Sheffield, U.K. Experimental work on the optical properties of photonic crystal waveguides resulted in several publications regarding interesting aspects of photonic band structure, including photonic modes with zero group velocity. He was also involved in experiments on semiconductor microcavities from the design and characterization stage, up to angular resolved photoluminescence experiments that revealed polariton redistribution by stimulated scattering under CW excitation. Following his Ph.D., he took up his current position in 2000 at Toshiba Research Europe Limited, Cambridge, U.K., where he has published several papers on single photon sources for quantum information technology.